Correlation between alignment geometries and memory effect in a surface-stabilized ferroelectric liquid crystal

Suraj Kumar,[1,2] Lokesh K. Gangwar,[1,2] Ambika Bawa,[1,2] Amit Choudhary,[3,*] Rajesh,[1,2] Surinder P. Singh,[1,2] and Ashok M. Biradar[2,†]

[1]*CSIR-National Physical Laboratory, Dr. K. S. Krishnan Marg, New Delhi-110012, India*

[2]*Academy of Scientific and Innovative Research (AcSIR), Ghaziabad-201002, India*

[3]*Physics Department, Deshbandhu College (University of Delhi), Kalkaji, New Delhi-110019, India*

(Received 9 June 2020; accepted 8 September 2020; published 28 September 2020; corrected 26 April 2022)

Memory effect in weakly aligned surface stabilized ferroelectric liquid crystal (SSFLC) material has been investigated by electro-optical and dielectric spectroscopy in three configurations of alignment: antiparallel, 90° twisted, and unaligned planar samples. It has been observed that two types of molecular dynamics exist in antiparallel rubbed cell in which memory effect is observed for longer duration than in other samples. One dielectric relaxation process is near the surface of the electrode and a second is in the bulk of the SSFLC. Both the molecular dynamics contribute in the switching process and affect the memory phenomenon in surface stabilized geometries. However, a single dielectric process is observed in twisted geometry in which the sample is showing shorter memory effect than in antiparallel and this is compared with unaligned samples also having cell thickness less than the pitch value of FLC. In an unaligned sample, a single dielectric process is observed and the smaple does not show memory effect at all. The investigation is significant to understand the anomalies occurring in memory observations in various geometries.

DOI: 10.1103/PhysRevE.102.032703

I. INTRODUCTION

The superiority of ferroelectric liquid crystals (FLCs) over their counterpart nematic liquid crystals is that they exhibit shorter switching time and memory effect. Memory effect in FLCs was one of the highly anticipated discoveries in the 1980s for its practical applications by manipulating a simple geometry with cell thickness less than the pitch value of the FLC material, called surface stabilizing effect [1]. It was found that the helical unwinding in surface stabilized samples was realized due to the fact that the energy required to unwind the helix by surface effect is low in thin sample cells as compared to thick sample cells having thickness more than the pitch value and resulting into the formation of two domains with opposite spontaneous polarization states [1]. The originally proposed critical parameter for the bistability (memory) in surface stabilized FLC (SSFLC) geometry was assumed to be the thickness of the sample itself. Later on, many other parameters were found to influence SSFLC structure. These factors included crystallinity of alignment layer [2], thickness and conductivity of alignment layer [3,4], chevron defect structures [5], and spontaneous polarization along with polar surface anchoring of alignment layer [6]. Other studies included the difference between pretilt angles of two antiparallel rubbed polymers to make zigzag defect-free SSFLC cell [7], bookshelf and chevron bulk structures [8], uniform SSFLC structure by obliquely evaporated silicon monoxide thin film [9], and strong memory in SSFLC state with polar anchoring strength of FLC on low concentration of polymer in rubbed polyimide layer alignment [10]. Solitary wave excitation is studied for the influence on electro-optical of SSFLC cell at various electric field values, temperature, and sample thicknesses [11,12]. Magnetic nanoparticles doping in SSFLC geometry has shown to affect Fréedericksz transition threshold of electric and magnetic fields due to the polarization and orientational behaviour of nanoparticles in FLC matrix [13]. The expansion series in powers of relevant order parameter tilt angle of Landau-de-Gennes free energy density is used to understand the thermodynamical properties of FLC material in SSFLC geometry [14]. Recently, numerious parameters of SSFLC geometry have been explored including biaxial surface potential and spatial resolution for wide field of view holographic displays [15,16].

In contradiction to the memory observed in sample cells having SSFLC geometry, the memory effect has also been observed in the samples where the spacing between the electrodes is more than the helical pitch length of the conventional (∼2–10 μm) and short pitch (0.3–0.8 μm) FLC materials. The short pitch FLC is also called as deformed helix FLC (DHFLC) because the helix can be deformed on the application of weak electric field before complete unwinding at a field more than the threshold value. In conventional FLCs, the sample showed the memory that is independent of sample cell gap between the electrodes and also showed the electroclinic effect near ferro to paraelectric phase transition [17,18]. The molecular arrangement at the phase transition (T_c) is identified as a de Vries type which is later considered as the root cause of memory effect in such FLC materials [19–21]. However,

*amitnpl2005@gmail.com; achoudhary@db.du.ac.in

†abiradarnpl@gmail.com

the DHFLC materials (helical pitch value ∼0.3–0.8 μm) have also been identified as materials that exhibit bistability phenomenon. In spite of SSFLC geometry, these short pitch FLC materials have shown memory effect in the non-SSFLC cell structure [22–28]. Even after contradictory results of memory effect, it has been continuously studied for their potential to be applied in practical applications.

However to avoid the rubbing of polymer constraint, the alignment for memory effect has also been achieved by shearing technique [29]. The main problem with shearing technique is that one cannot get a uniform planar alignment over the large display area. The only technique to get a uniform alignment over the large area is the rubbing of polymer-coated substrates. Researchers all over the world, including our own group has published many research findings based on the memory effect in SSFLCs in the last three decades, but still the perfect memory effect could not be produced due to their nonrepeatability, stability, and incomplete understanding of molecular dynamics. The main issue with polymer rubbed surfaces that hinder the process of obtaining the perfect memory in FLCs is the surface anchoring phenomenon. Recently, it has been predicted by our group that in the medium thickness sample cells (∼4–20 μm) with polymer rubbed surfaces, two dielectric relaxation processes exist which affects the basic characteristics of the FLC material. One dielectric process near the surface of the electrodes which is partially unwound and second process in the bulk of the cell which is completely wound, resulting into two phenomena as observed by dielectric and electro-optical studies [30–33]. Of course, these two relaxation processes depend on the FLC material parameters also such as spontaneous polarization, pitch value, surface anchoring, and viscosity *etc*.

In the present paper, we investigate the molecular dynamical behaviour of three SSFLC cells, namely, antiparallel, twisted aligned (90° angle), and unaligned sample cells for the memory effect. All the aligned samples (antiparallel and twisted) are fabricated using weakly rubbed polymer thin film over the indium tin oxide (ITO)-coated glass plates. A prominent memory effect is realized in antiparallel sample, whereas a weaker memory is observed in twisted SSFLC sample. However, no memory has been observed in the unaligned sample as per the investigation by dielectric and electro-optical studies. It has also been observed that two separate dielectric relaxation peaks, associated with two dielectric processes, are seen in antiparallel rubbed planar aligned cell due to Goldstone mode (GM) and partially unwound structure (*p*-UHM), whereas only one dielectric relaxation peak is observed in twisted and planar multidomain (unaligned) cell of surfaces stabilized geometry. The role of helical structure is predicted even after the unwinding of helical structure by surface effect. The effect of temperature in all the cells has been investigated for deeper analysis.

II. EXPERIMENTAL

All the sample cells having surface stabilized geometric conditions (also called as SSFLC cells) were prepared by using highly conducting and transparent ITO-coated glass plates having sheet resistance of ∼20 Ω/□. The desired electrode patterns of thin ITO film of dimensions 4×4 mm were prepared using photolithographic technique. The ITO pattern electrodes were coated with polymer nylon 6/6 by spin coating and were rubbed ten times along the desired direction using the valvet cloth for the alignment of FLC molecules. The ten repetitions of rubbing are sufficient to provide the weak anchoring of FLC molecules on the alignment layer. Weak and strong rubbed surfaces were previously optimized using contact angle and atomic force microscopy (AFM) measurements which are reported in our previous study [32]. It was found that ten repetitions of rubbing is attributed to weakly rubbed cells and the contact angle increased up to 40 repetitions attributing to strongly rubbed cells. As the number of rubbing repetitions was further increased beyond 40, the grooves visualization was found to be reduced and the contact angle was found increasing slowly which indicates toward the little modification in the surface morphology.

The ITO patterned thin film substrates were assembled in the form of parallel plate capacitor facing each electrode inside the enclosed area and separated by placing the Mylar spacer of 3.5 μm thickness between the two plates in the nonconducting region of the substrates. The FLC material, SCE-13 (BDH, England), was inserted into all the cells by means of capillary suction at temperatures above its isotropic phase 115°C. The electrical connections were taken out from the electrodes by soldering the copper wire on them using indium metal as a soldering materials to reduce the contact resistance between the ITO film and connecting wires. These connecting wires were used for applying the electric field on the sample cells through electrodes. The phase sequence of the used FLC material is as

$$\text{Cryst.} \overset{-20\,^{\circ}\text{C}}{\leftrightarrow} \text{Sm}C^{*} \overset{61\,^{\circ}\text{C}}{\leftrightarrow} \text{Sm}A^{*} \overset{91\,^{\circ}\text{C}}{\leftrightarrow} N \overset{115\,^{\circ}\text{C}}{\leftrightarrow} \text{Isotropic}.$$

Here "Cryst." represents the crystalline phase of SCE-13 material. Sm*C**, Sm*A**, and *N* are the representations of chiral smectic *C*, chiral smectic *A*, and nematic phases of FLC, respectively.

The alignment of FLC molecules was examined under the cross polarized optical microscope (Carl Zeiss, Axioskop-40A Pol, Germany). The dielectric measurements were conducted by using impedance analyzer (Wayne Kerr, 6540A, precision impedance analyzer, UK, frequency range 20 Hz to 120 MHz) in the frequency range of 20 Hz to 1 MHz. The measurements were carried out at different probing AC and DC voltages at different temperatures by using hot stage (Julabo 25 HE, Germany) having the temperature stability of ±0.1°C.

As the FLC material possesses the helical pitch value of 10 μm, therefore, the surface stabilized cell of ∼3.5 μm spacing between the two substrates (also called as thickness of the sample cell) were prepared. Three types of cells were prepared by using the above described method. In the first type, the antiparallel rubbed surfaces were assembled. In the second type, one of the electrodes was given 90° rubbing direction and called as twisted geometry. In the third type of cell, no rubbing was applied to the nylon 6/6 coated ITO substrates on any of the electrodes and multidomain planar cell was obtained by slow cooling process. The planar alignment in all the three types of cell was analyzed by polarized optical microscopy and then the dielectric measurements were performed for detailed study.

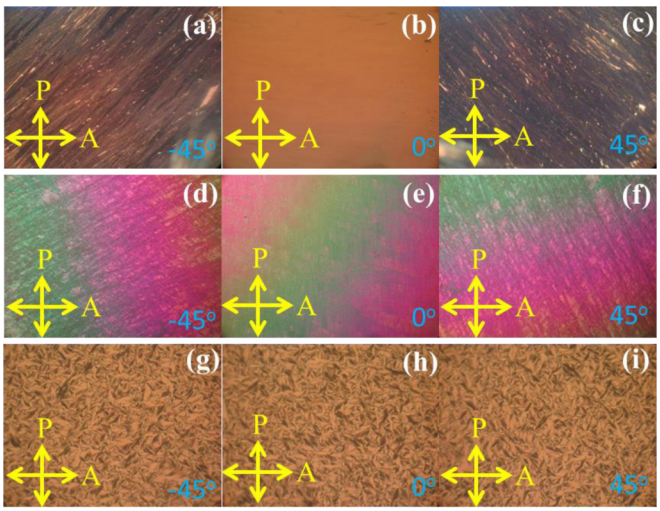

FIG. 1. Optical micrographs at 10 V DC voltage for surface stabilized geometry of antiparallel rubbed cell having rubbing direction at (a) −45°, (b) 0°, and (c) 45° with respect to polarizer. In twisted structure SSFLC cell having rubbing direction (d) in scattered state at −45°, (e) 0°, and (f) 45°. In no rubbing SSFLC cell (g) in scattered state at −45°, (h) 0°, and (i) 45° angles with respect to polarizer. These measurements have been performed at 30°C in Sm*C** phase. The crossed double headed arrows indicates the positions of polarizer (P) and analyzer (A).

III. RESULTS AND DISCUSSION

A. Optical observation

Recently, it has been observed by us that in perfectly planar aligned and strongly anchored cells having the medium thickness range (∼5-20 μm), the cell consists of two dielectric relaxation processes: one is near the electrode surface due to partially unwound helical structure and second process is in the bulk of the cell which is completely in the helical wound state [30–33]. If the thickness of the cell is more than the pitch value of the FLC material and the anchoring is strong, then it would be difficult to form a single relaxation process [24]. Therefore, in the present investigation, the cell thickness is maintained less than the pitch value of the FLC material and anchoring is kept weak by providing few number of rubbing strokes (ten numbers) by using valvet cloth on the polymer-coated surface for the alignment to establish single relaxation process and to study the molecular dynamics in SSFLC geometry. This geometry of cell leads to a fabrication of SSFLC device which is expected to exhibit the memory effect.

Before memory effect analysis of all the samples, a voltage of 10 V is applied to each sample to unwind the helical structure and bring all the molecular orientation to unidirection so that the difference in the texture could be analyzed with no confusion. In the first type of cell, parallel rubbing was done and assembled in antiparallel direction of rubbing, the perfect planar alignment of FLC molecules is observed from bottom to the top surface of the cell by looking at the textures obtained through the transmission studies under crossed polarized optical microscope (Fig. 1). Figure 1(a) shows the texture when rubbing direction is kept at −45° with respect to optic axis of polarizer, whereas Figs. 1(b) and 1(c) are at 0° and 45° angles, respectively. This confirms that the alignment is planar and unidirection. As seen in Figs. 1(d)–1(f), sample cells are assembled in twisted geometry where the rubbing directions on both the electrodes are perpendicular to each other and nearly no difference is observed in the intensity of these textures. Also, these textures represent position of sample cell which is kept at −45° angle with respect to polarizer [Fig. 1(d)], parallel state with respect to polarizer [Fig. 1(e)], and 45° angle rotated state with respect to polarizer [Fig. 1(f)]. No variation in the intensity of these states suggests that the alignment provided to FLC cell is twisted in surface stabilized geometry. In the third type of cell, where there is no rubbing on either of the electrode, the multidomain alignment is seen in the optical micrographs as shown in Figs. 1(g)–1(h). The orientational effect could be realized by focusing on one of domains in the texture. The orientation based analysis of unaligned sample suggests that the alignment is parallel but overall intensity is not changing with rotation of the cell due to random orientation of molecular director of the domains. Also, as can be seen from the texture, no dechiralizarion lines are observed, suggesting that the helix is completely unwound due to the surface constraints imposed by maintaining the thickness of the cell less than the pitch value of material. The observation confirms the material is in surface stabilized effect. Since there is no preferred direction given to the molecular alignment of the material, no chevron type or bookshelf structures are observed. However, it should be noted, that the bookshelf type of structures are also not observed in the other two samples as well. This is due to the fact that the rubbing strength is maintained very weak. However, the lines along the rubbing direction caused by bookshelf geometry could be realized in antiparallel sample which confirms the SSFLC state of the sample.

The optical texture studies confirmed the surface stabilized geometry for all the samples. The other most noticeable aspect of SSFLC geometry is the bistability (memory) effect which is studied in all these samples. If one examines the memory effect in all the three types of surface stabilized geometries, then the optical memory is observed in antiparallel rubbed cell [Fig. 2(a)] only when DC bias voltage of 10 V is applied, and starts degrading after two minutes of removal of DC field, as seen in Fig. 2(b). Here in antiparallel sample, the memory is retained for two minutes. In twisted aligned cell [Figs. 2(c) and 2(d)], the optical memory is not observed in the textures. As the smectic layers are twisted by 90° angle of rubbing from bottom to top surface of the cell, the loss in memory is due to the fact that the restoring force is applied by the twisting alignment anchoring on the substrate. In multidomain cell, the memory effect could not be realised due to different domains in all possible orientations which resulted in to no net optical change in the transmission as seen in Figs. 2(e) and 2(f). Memory could not be observed even after critical focusing on a single domain.

B. Dielectric spectroscopy investigation

Memory effect in various cell structures (antiparallel, twisted, and unaligned samples) is further investigated by using dielectric spectroscopy. The comparative quantitative

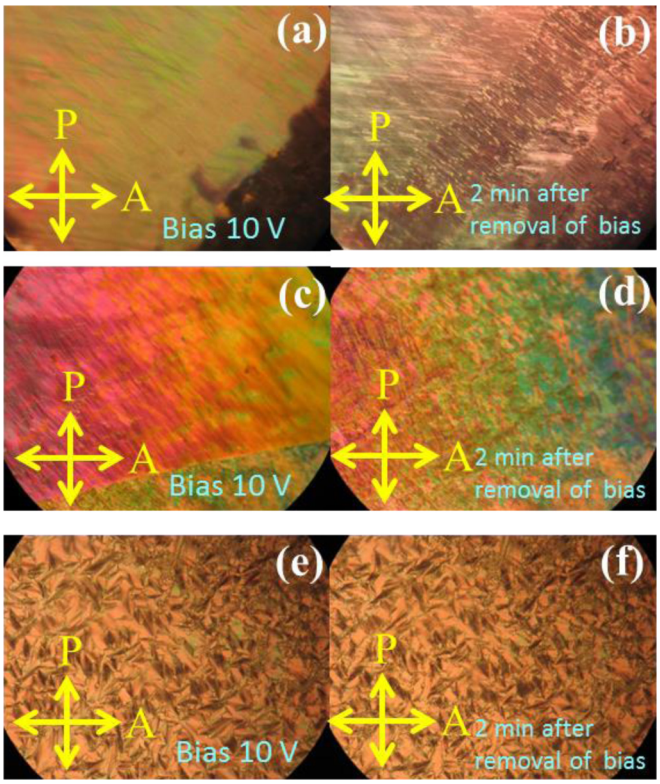

FIG. 2. Optical micrographs of surface stabilized geometry cell of antiparallel rubbed cell (a) with 10 V and (b) 2 min after removal of bias. Twisted SSFLC cell (c) with 10 V and (d) 2 min after removal of bias. Unaligned cell (e) with 10 V, and (f) 2 min after removal of bias. These measurements have been performed at 30°C in SmC^* phase. The crossed double headed arrows indicates the positions of polarizer (P) and analyzer (A).

memory effect is analyzed using dielectric spectroscopy technique by scanning each sample from 20 Hz to 1 MHz frequency and values of relative permittivity are selected at 60 Hz for the analysis of memory phenomenon as shown in Fig. 3(a). The low frequency 60 Hz is sufficiently below the relaxation frequency of any collective dielectric relaxation process at which the dipoles can sufficiently respond to the applied electric field. The relative permittivity value at 60 Hz is enough to exhibit the dipolar response at 800 mV applied probing AC voltage. The comparative memory (M_c) effect is analyzed by data storage capacity and compared with the relative dielectric permittivity of each sample with antiparallel at 60 Hz frequency by using the relation

$$M_c\% = \delta\varepsilon_i'(60) \times 100/\varepsilon'_{0V,\text{anti}-\text{parallel}}(60), \quad \text{where}$$
$$\delta\varepsilon_i'(60) = \varepsilon'_{0V}(60) - \varepsilon_i'(60).$$

Here, $M_c\%$ is the comparative memory effect in percentage. ε' is the dielectric permittivity. $\delta\varepsilon_i'(60)$ is the permittivity difference at 60 Hz between the initial state (unbiased state) and other states (biased, just after removing bias field, and 2 min after removing DC bias). 'i' stands for the various bias and after bias states. Here, there are four such states as 0 V (initial state), with bias, just after removal of bias, and 2 min after removal of bias. $\varepsilon'_{0V}(60)$ is the permittivity value at 0 V bias (initial state before applying bias) at 60 Hz frequency for different cells. $\varepsilon_i'(60)$ is the permittivity value at i^{th} state at 60 Hz frequency. $\varepsilon'_{0V,\text{anti}-\text{parallel}}(60)$ is the permittivity of antiparallel cell at 0 V bias (initial state) and at 60 Hz frequency with which the memory of all other cells are compared.

Figure 3(a) reveals the comparative data storage (a comparative memory effect, $M_c\%$) for all the three samples and is analyzed with the help of percentage variation in dielectric permittivity value. In the presence of DC electric field, dielectric permittivity shows suppressed dielectric properties and gives information of signal given to the sample cell, which is to be stored in the cell. If there is a perfect memory effect, then there is no loss of data and we call it 100% memory. Initially for a virgin cell (when no field is applied), it is presumed that at this instance, the samples are not in memory state. On the application of electric field, the sample switches to one of the switching states and is assumed to possess 100% memory in antiparallel sample for reference to other samples. This is assumed 100% memory state and an ideal memory storage if no data is lost after removal of electric field. All the memory states for an antiparallel sample cell is analyzed in comparison to this 100% memory state. Now, just after the removal of electric bias field, the sample starts losing its dielectric property of switched state (memory state) but still has not attained the exact initial state, that is why the states are assumed to be in partial memory states. The memory effect is lost with time as observed after 2 min duration of removal of electric field and almost all the samples show memory loss up to large extent. However, antiparallel sample stores 31% data after 2 min of removing the electric field, whereas, twisted sample stores mere 8.6% data. However, unaligned sample exhibits a contradictory behaviour after 2 min of removal of electric field. The FLC material is observed to have negative dielectric permittivity difference due to depolarization field which forces the molecules to a reverse switching state, Fig. 3(a). Because of this reason, the sample attains the permittivity value more than the initial value of this sample and leads to a negative effect in memory by switching the molecules in reversed state. The results indicate that the antiparallel sample is capable to show longer duration memory effect. However, as can be seen from the data recorded just after the field was removed, samples tend to lose their memory almost immediately after removing the electric field in planarly multidomain cell, thereby implying that memory observed in SSFLC devices of such geometry is not suitable for data storage devices.

The imaginary part of complex dielectric constant (dielectric loss, ε'') studies have also shown the evidence of shifting of relaxation process during the electrical signal storage and has a relation with memory states. The ε'' is calculated by using the data of tanδ multiplied by real part of the complex dielectric permittivity (tan$\delta = \varepsilon''/\varepsilon'$) and the relaxation frequency is calculated by using $\nu_{\varepsilon''} = \nu_{\tan\delta} * \sqrt{\varepsilon'(\infty)/\varepsilon'(0)}$, where $\nu_{\varepsilon''}$ and $\nu_{\tan\delta}$ are the peak frequency values are taken from ε'' and tanδ curves, respectively. $\varepsilon'(\infty)$ and $\varepsilon'(0)$ are the values from real part of complex dielectric permittivty at high frequency (a high enough where ε' is not affected with increase in frequency) and low frequency (a low enough frequency where permittivity is almost stagnant and is not changing with frequency), respectively [34]. It is natural to observe a shift in dielectric relaxation process when electric

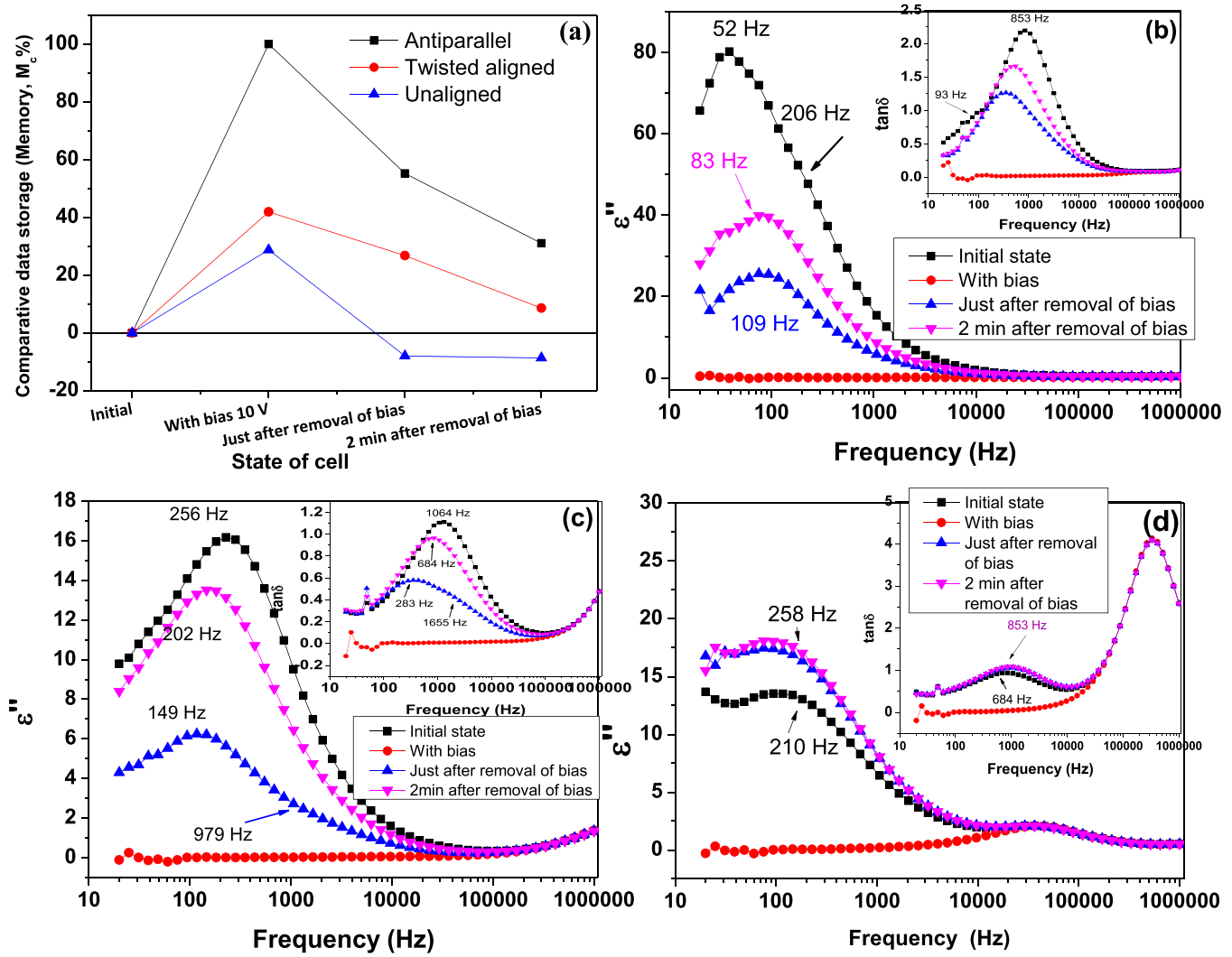

FIG. 3. (a) Comparative data storage response (memory effect) for all the three samples with applied DC field in SmC^* phase. Dielectric loss (ε'', imaginary part of complex dielectric constant) as a function of frequency without and with DC bias for (b) antiparallel, (c) twisted cell, and (d) unaligned cells. Insets of all the figures show tanδ as a function of frequency of corresponding cell.

or physical constraints are applied to the FLC material. In the present case, constraints due to surface stabilization of the sample in the confined geometry leads to the surface stabilized structure which further leads to bookshelf geometry and resulting the material into physical constraint and second constraint is due to the applied electric field which restricts the molecules to a switching state. Initially when no field is applied, the dielectric loss (ε'') shows the existence of two processes, marked at 206 Hz (GM) and at 52 Hz (p-UHM) frequencies as can be seen from the inset of Fig. 3(b) also. The initial magnitude of the peak of tanδ is more than 1 which is unusual in the context of dielectric spectroscopy but such results can be observed if some parasitic effects appear in the cell [35]. Here, the high value of tanδ is due to existence of surface effect p-UHM. As also seen in Fig. 3(b), the relaxation peak of ε'' is completely suppressed on the application of DC bias voltage and is not observable in the plot, however, as soon as the field is removed from the sample, the relaxation peak starts appearing again and keeps on shifting the peak mangnitude to the initial state that is toward the higher frequency side, implying that the sample is losing memory state. Otherwise, if the memory was long lasting, then we could have expected the relaxation process of materials and consequently fixed relaxation peak at the same frequency position. However, the peaks are continuously shifting toward the initial frequency values resulting into the dynamical orientation of molecules to the relaxing initial state. It is one of the marking of memory identification in such SSFLC samples. In the present samples, the degradation in memory state is recorded continuously.

In another observation from inset of Fig. 3(b), the tanδ peak is observed to be asymmetrical when recorded immediately after the removal of electric field and tends to get symmetrical as the molecules present in the sample attempt to acquire their initial state. This indicates toward the nonuniform behaviour of the molecular arrangement to the applied probing electric field in the whole sample. It has also been observed by us recently that the FLC molecules could be arranged in two dielectric processes in nonSSFLC sample cell. This is based on the fact that if the anchoring of the molecules is made strong enough to generate two dielectric processes, one process is at

the interface of FLC and alignment layer over the electrodes whereas another is the in the bulk of FLC material itself [30]. In the present samples with antiparallel and twisted alignment, the same kind of behavior seems to appear immediately after removal of DC bias field as observed in Figs. 3(b) and 3(c). As seen in Fig. 3(c), the twisted sample has also exhibited the faster memory loss than the antiparallel sample. Again, the observation of two relaxation process can be easily realized in the curve that was recorded immediately after the removal of DC bias in which the dielectric process observed at lower frequency ∼149 Hz is due to the surface effect whereas the other at around 979 Hz is due to the usually observed GM process. After 2 min, the resultant relaxation peak is shifted toward the GM process and tends to attain its initial state. The same information can be realized in the tanδ curves shown in inset of Fig. 3(c) also.

However, only one relaxation peak is observed at lower frequency range in unaligned cell having the same thickness as in antiparallel and twisted cells. However, for higher frequencies at around 40 kHz in ε'' and 331.5 kHz in tanδ curves, a separate peak is seen in unaligned cell unlike in other two geometries as seen in Fig. 3(d). This high frequency peak is far away from *p*-UHM or GM relaxation peaks which could be due to some artifacts in the unaligned cell or can be molecular process around short axis of the molecule as the cell is unaligned. This high relaxation process is independent of AC or DC bias electric field suggesting the nonmolecular dielectric process. However, this peak is not observed in antiparallel or twisted geometries, therefore it is difficult to say that it can be related to the ITO resistence. The dynamics of this dielectric process can be understood in bulky FLC material cell as reported by Gupta *et al.* [36], where the thickness of the cell is high enough.

Initially with no DC bias in Fig. 3(d), the peak at around 200 Hz is suppressed on application of 10 V DC bias on the same sample. The ε'' curve attains the same values immediately after the removal of bias field. This aspect has also been realized in tanδ curves as shown in inset of Fig. 3(d) also where this peak is around 684 Hz. In this case, it could be immediately estimated that the availability of GM process and absence of lower frequency process differs from other two samples on the grounds of surface effects. This means the lower frequency relaxation process (*p*-UHM) other than the GM is caused by the surface interface with FLC only.

Further analysis of the behavior of the FLC molecules which are responsible for degradation of the memory effect, is performed by dielectric spectroscopy. Figure 4 shows ε'' measurements at different probing AC voltages in all the three type of cells. As seen in Fig. 4(a), the two peaks are clearly seen from the curves of ε'' for higher probing AC voltages and the low frequency process later masks the GM process peak. One of the relaxation peaks is due to GM which is almost independent of probing AC voltage and second peak at lower frequency than GM is due to *p*-UHM attributing toward the contribution of the surface molecules which is highly dependent on probing field [24]. The same information can be inferred from the tanδ curves as shown in inset of Fig. 4(a). This means that there exists two dielectric processes, one near the surface of the electrodes and second in the bulk of the sample cell. This clearly indicates that the helical twist

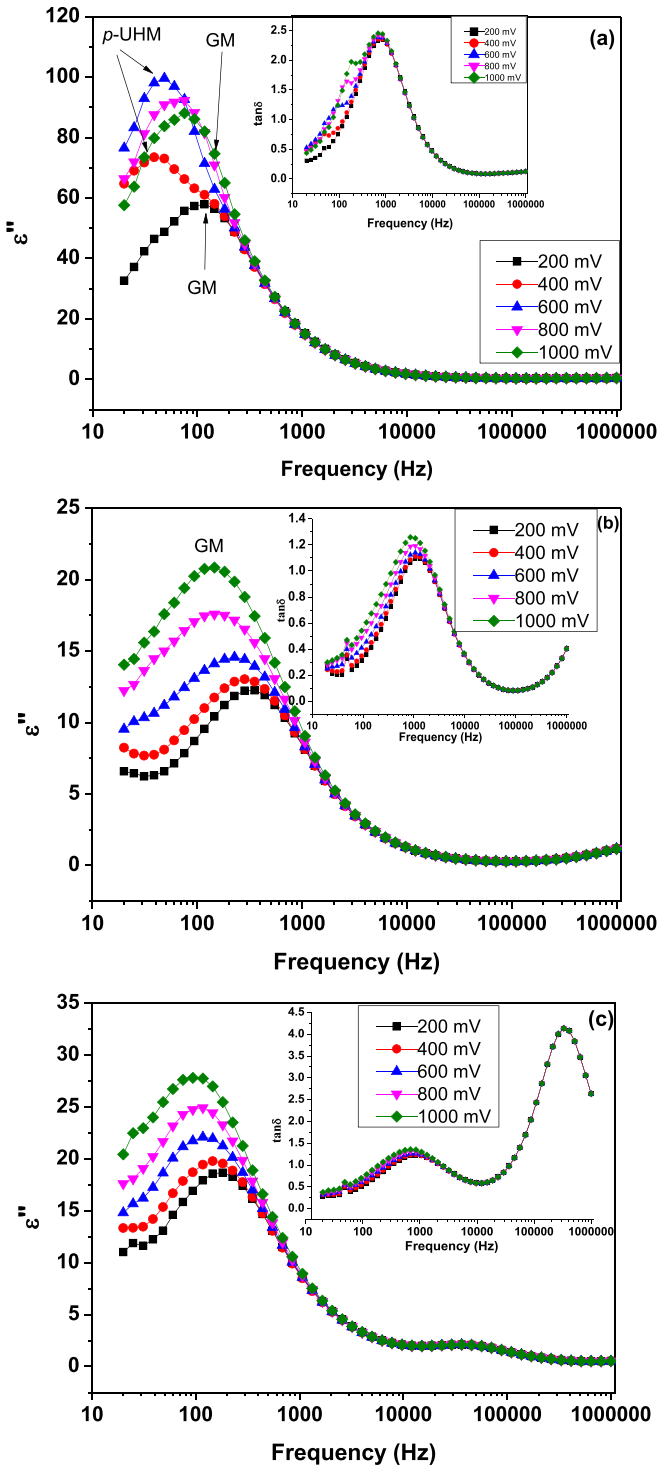

FIG. 4. Dielectric loss (ε'') as a function of frequency of FLC in SmC* phase with different probing voltages at room temperature in (a) antiparallel, (b) twisted, and (c) unaligned sample of surface stabilized geometries. Insets of all the figures show tanδ as a function of frequency with different probing AC voltages of corresponding cell.

near the surface of the electrodes is contributing distinctly in comparison to the bulk of FLC in the cell. This presence of *p*-UHM near the electrode and GM process in the bulk of FLC are the two parts of the same FLC material in the SSFLC

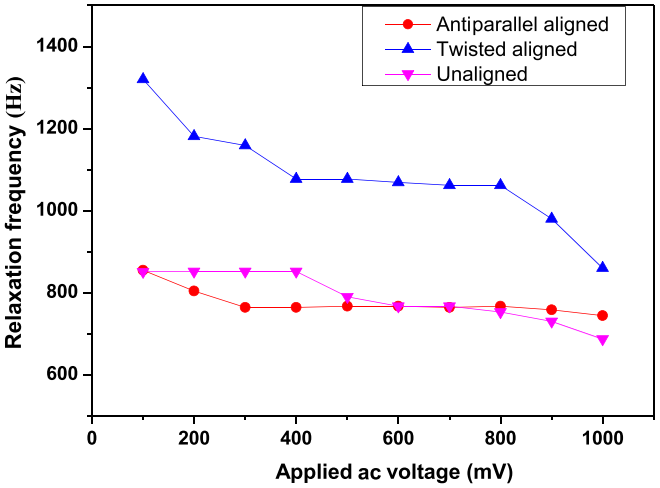

FIG. 5. Relaxation frequency of GM in Sm*C** phase at different amplitudes of probing AC voltage at room temperature in (a) antiparallel, (b) twisted, and (c) unaligned cells.

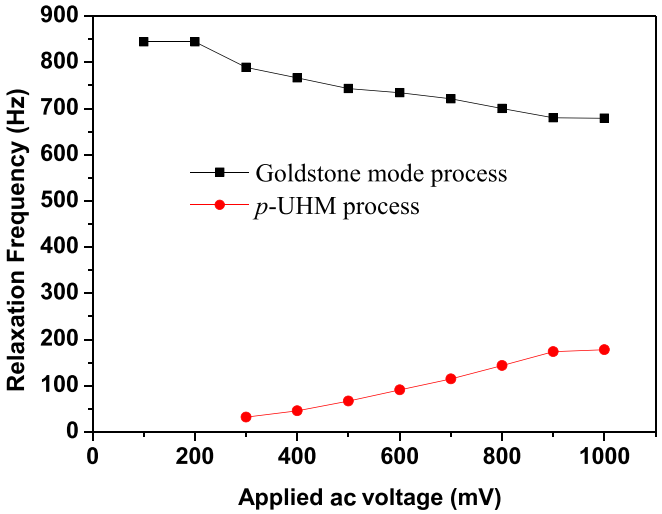

FIG. 6. Relaxation frequency of GM and *p*-UHM processes in Sm*C** phase as a function of probing voltage at room temperature in antiparallel rubbed cell.

cell. The *p*-UHM persists at almost all the levels of probing AC voltages. However, at low amplitude of AC voltage, the *p*-UHM exists at reduced frequency and at increased AC amplitudes where it exists at frequency close to the frequency of GM.

In twisted geometry cell, only one peak in ε'' versus frequency data is observed due to the GM because there is only one dielectric process of twisted structure from the bottom to the top surface as seen in Fig. 4(b) and its corresponding inset and similar is the case in multidomain (unaligned) planar cell [Fig. 4(c)]. It is worth pointing out here that the presence of distinct behaviour of surface molecules is also reflected on the left-hand side of the ε'' curves of twisted and multidomain cell with increase in the probing AC voltage. However, the *p*-UHM peak is very difficult to be resolved in the twisted cell structure. The two dielectric processes (GM as well as lower frequency mode, *p*-UHM) have been observed when observing memory effect in the twisted sample as can be seen in the curve obtained just after the removal of DC bias in Fig. 3(c). However, the same is not reflected here in the data of unbiased sample at any level of probing AC voltage, Fig. 4(b). The role of surface is depicted by the *p*-UHM process which is more dominating in the antiparallel than in twisted sample. In antiparallel sample, the presence of *p*-UHM reveals the helical unwinding at the interface of the FLC and alignment layer whereas in twisted sample, the two dielectric processes have been observed in the state of immediatly after removal of bias field, Fig. 3(c). No such two processes have been realized in unaligned multidomain sample in any condition of bias as there is no rubbing provided at the alignment layer which means no major role the surface effect is expected in this cell, resulting in the multidomain formation.

Figure 5 shows the relaxation frequency of the GM in all the three types of cells with different probing AC voltages at room temperature. The relaxation frequency of GM is almost independent of applied field in antiparallel cell whereas in twisted and multidomain planar cells, it decreases with increasing applied probing AC field. The relaxation frequency of GM in antiparallel cell is independent of probing field because of the fact that the two processes (GM and *p*-UHM) are completely separated as shown in Fig. 4(a) and its corresponding inset. In twisted and unaligned cells, there might be some contribution of surface FLC molecular dynamics, resulting in the decrease in relaxation frequency of GM with increase in probing AC field.

Figure 6 shows the relaxation frequencies of two processes in the sample cell of antiparallel alignment due to two well separated dielectric relaxation processes, one is due to surface effect which partially unwind the helical structure (*p*-UHM) and second is due to the bulk in which the collective phase fluctuations of molecules (GM) occurs in the sample cell. As seen in the figure, the relaxation frequency of GM is found decreasing whereas relaxation frequency of *p*-UHM increases with increasing applied probing AC field. However recently, it has been observed that under specific condition of natural cooling of the sample having cell thickness of $\sim 8\ \mu$m, the *p*-UHM process is not observed in twisted samples as a function of applied AC voltage at room temperature [37].

The set of three samples (antiparallel, twisted 90°, and unaligned planar) has also been investigated by dielectric permittivity data by applying various amplitudes of applied probing AC voltage, Fig. 7. The presence of two processes in the antiparallel planar cell is also seen in the permittivity curves as shown in Fig. 7(a). The permittivity value at frequencies less than 1 kHz is almost double for antiparallel cell, Fig. 7(a), as compared to the twisted and unaligned sample cells due to the presence of two dielectric relaxation processes in surface stabilized geometry. The permittivity increases with probing AC field in twisted [Fig. 7(b)] and multi domain samples [Fig. 7(c)], whereas in the antiparallel sample, the permittivity is not affected much due to the presence of two dielectric processes in the cell [Fig. 7(a)]. The high value in permittivity with probing field for the antiparallel sample reveals the presence of two dielectric processes whereas in twisted and unaligned, the lower permittivity indicates the weak or no presence of *p*-UHM process along with GM.

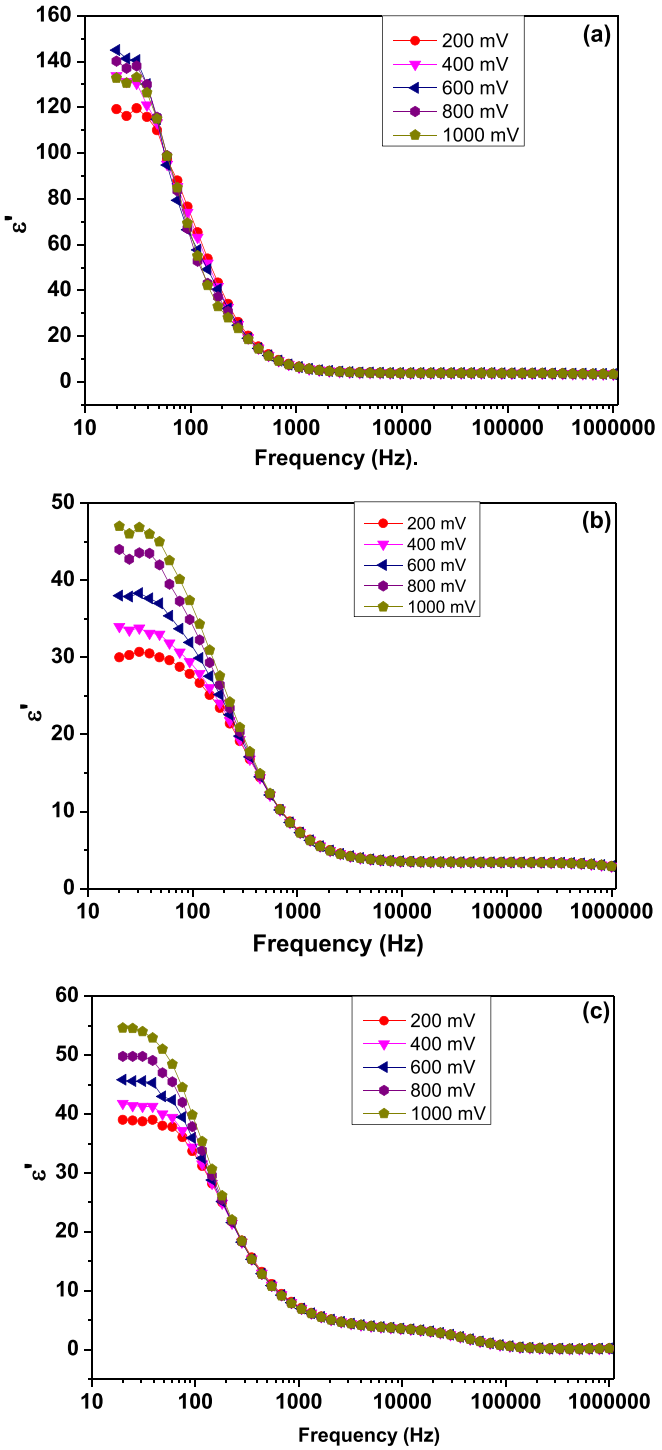

FIG. 7. Dielectric permittivity as a function of frequency in Sm*C** phase at different probing voltages at room temperature in (a) antiparallel, (b) twisted, and (c) unaligned cells.

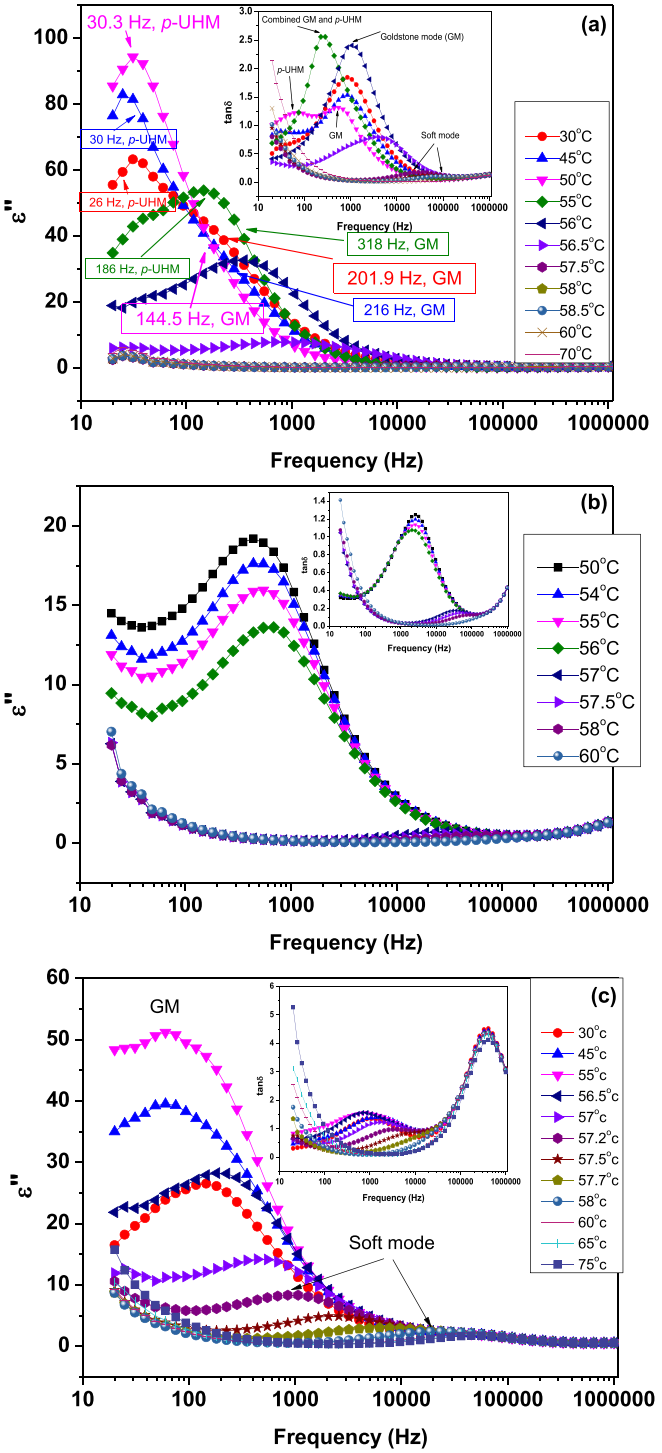

FIG. 8. Dielectric loss (ε'') response of cell as a function of frequency in Sm*C** phase at 800 mV probing AC voltage at different temperatures in (a) antiparallel, (b) twisted, and (c) unaligned cells in Sm*C** and Sm*A** phases.

Figure 8 shows the ε'' versus frequency at different temperatures in all the three type of cells in surface stabilized geometries at probing amplitude of 800 mV. As seen in the antiparallel rubbed cell [Fig. 8(a)], the ε'' curves are asymmetric because of the two dielectric relaxation processes. This is due to the surface anchored and bulk relaxation processes which are having different characteristic times with temperature and amplitude of probing AC voltage. The ε'' attains maximum value at 50 °C where two processes exists at 144.5 and 30.3 Hz frequencies. Two processes can be estimated from tanδ curves also as shown in inset of Fig. 8(a). After the T_c from Sm*C** to Sm*A**, the least frequency process contribution is disappeared indicating that it was associated with the Sm*C** phase

and surface effect only. At room temperature (∼30°C), the GM (phason mode) caused by bulk FLC molecules is clearly identified at frequency ∼201.9 Hz but the relaxation process caused by surface partial unwound helical structure is extimated at 26 Hz. On increasing the temperature, the low frequency process becomes dominating at 50 °C which near phase transition temperature (T_c) becomes weak and finally disappears at 56 °C before transition to SmA* phase.

The dielectric relaxation process related to surface molecules is dependent on probing AC voltage and temperature whereas the GM dielectric process is caused by the molecules collectively in the bulk of FLC material which is independent of probing AC voltage and temperature in SmC* phase [32]. Therefore, in literature there is no consistent behaviour of GM with temperature. Also, the transition temperature of SmC*-SmA* of FLC is expected to be low in thin cells as compared to in thick cells [38]. The same is applicable for this FLC material also and the phase transition is expected to remain less than the shown in experimental section for this materials due to the surface effect. As can be seen in Fig. 8, the transition temperature is observed at ∼57.5°C whereas its bulk phase transition in thick cells is 61°C as mentioned in the phase sequence of this FLC material. As shown in the [Fig. 8(a)], if one considers the curves at 50, 55 and 56°C temperatures, the GM and p-UHM process can be seen clearly at 50°C whereas at 55°C temperature, p-UHM process is dominant and overshadows the GM. At 56.5°C, the GM overshadows the p-UHM process suggesting that the dynamical response of both dielectric processes have become uniform. In the twisted alignment cell Fig. 8(b), only one relaxation peak due to GM process is seen and behaves almost independent of temperature till phase transition from ferro to paraelectric phase at 57°C, which could be due to the fact that there is only one dielectric process existing overall in the twisted structure. In multidomain planar cell, the GM dielectric relaxation frequency slightly increases with temperature and finally gets converted into the soft-mode process after the transition temperature of SmC* to SmA* phase at 57.2°C as shown in [Fig. 8(c)]. It is worth to point out in multidomain cell, the dielectric relaxation frequency continuously increases with temperature from deep SmC* phase as GM and even in the SmA* phase as Soft mode. The process at ∼40 kHz and 300 kHz frequency in ε'' and tanδ, respectively, in Fig. 8(c), as observed in Fig. 3(d) also, is found independent of temperature suggesting rule out the possibility of molecular mode that it is not associated with dielectric relaxation process unlike in Ref. [36]. The behavior of FLC mateials in various geometries has shown the distinct behaviour for the observance of memory effect in all the three sample geometries. The anitparallel geometry has been found suitable for the memory effect in SSFLC state of the material.

IV. CONCLUSION

We have analyzed three alignment geometries in surface stabilized confinement samples of SCE-13 FLC. The rubbing strength for all the sample cells is kept weaker than the normal rubbing required in non-SSFLC cells. Memory effect is found for longer duration in the antiparallel sample than in the twisted and unaligned samples. The antiparallel aligned sample shows two dielectric relaxation processes, one is at the interface of FLC and alignment layer, called as p-UHM; and another is in the bulk of the FLC, normally called as GM dielectric process. The occurence of p-UHM has resulted in high dielectric constant. The contribution of p-UHM in antiparallel leads to large change in the dielectric properties during data storage which in turn takes longer time to return the ground state after the removal of bias field in comparison to the other two geometries. However, the p-UHM process is partially observed in twisted sample. In unaligned sample, the permittivity attains higher value than the ground state after removal of the bias field, suggesting the existence of a stronger depolarizing field, which tends to restore the molecules to ground state or even it may lead to the reverse switching state. In this comparison of the data storage capacities of three types of aligned samples, p-UHM-assisted antiparallel samples are more prominent than other alignment geometries. The study is promising for the choice of suitable cell geometries for the fabrication of data storage devices using FLC materials.

ACKNOWLEDGMENTS

We sincerely thank to Dr. D. K. Aswal, Director of the National Physical Laboratory, New Delhi, for his continuous encouragement in the work. Authors A.M.B. and A.B. are thankful to Council of Scientific and Industrial Research (CSIR), India [21(986)/13/EMR-II], New Delhi, for financial assistance under the emeritus scheme.

[1] N. A. Clark and S. T. Lagerwall, Appl. Phys. Lett. **36**, 899 (1980).
[2] W. J. A. M. Hartmann, A. M. M. Luyckx-Smolders, and R. P. v. Kessel, Appl. Phys. Lett. **55**, 1191 (1989).
[3] T. C. Chieu and K. H. Yang, Appl. Phys. Lett. **56**, 1326 (1990).
[4] T. C. Chieu, J. Appl. Phys. **69**, 8399 (1991).
[5] W. J. A. M. Hartmann and A. M. M. Luyckx-Smolders, J. Appl. Phys. **67**, 1253 (1990).
[6] N. Vaupotič and M. Čopič, Phys. Rev. E **68**, 061705 (2003).
[7] Y. Noguchi, N. Ito, and H. Furue, Ferroelectrics **365**, 27 (2008).
[8] A. Mochizuki, T. Makino, H. Shiroto, Y. Kiyota, and T. Yoshihara, Mol. Cryst. Liq. Cryst. Sci. Technol. Sect. A **303**, 391 (1997).
[9] S. Xiao, Y. Le, X. Zhou, and K. Xu, Mol. Cryst. Liq. Cryst. Sci. Technol. Sect. A **300**, 263 (1997).
[10] D. S. Seo, Liq. Cryst. **19**, 891 (1995).
[11] I. Śliwa, W. Jeżewski, W. Kuczyński, and J. Hoffmann, Phase Trans. **85**, 345 (2012).
[12] W. Jeżewski, W. Kuczyński, and J. Hoffmann, Phys. Rev. E **83**, 042701 (2011).
[13] S. Shoarinejad and A. Sadeghisahebzad, J. Mol. Liq. **220**, 1033 (2016).
[14] S. Singh, P. K. Tripathi, and S. Singh, J. Mol. Liq. **241**, 422 (2017).
[15] A. Kaznacheev, E. Pozhidaev, V. Rudyak, A. V. Emelyanenko, and A. Khokhlov, Phys. Rev. E **97**, 042703 (2018).

[16] Y. Isomae, S. Aso, J. Shibasaki, K. Aoshima, K. Machida, H. Kikuchi, T. Ishinabe, Y. Shibata, and H. Fujikake, Jpn. J. Appl. Phys. **59**, 040901 (2020).
[17] S. Kaur, A. K. Thakur, S. S. Bawa, and A. M. Biradar, Appl. Phys. Lett. **88**, 122905 (2006).
[18] A. Choudhary, S. Kaur, G. Singh, J. Prakash, A. K. Thakur, and A. M. Biradar, J. Appl. Phys. **101**, 074112 (2007).
[19] S. Kaur, A. K. Thakur, A. Choudhary, S. S. Bawa, A. M. Biradar, and S. Annapoorni, Appl. Phys. Lett. **87**, 102507 (2005).
[20] A. K. Thakur, A. Choudhary, S. Kaur, S. S. Bawa, and A. M. Biradar, J. Appl. Phys. **100**, 034104 (2006).
[21] G. Singh, A. Choudhary, S. Kaur, A. M. Biradar, and W. Haase, Jpn. J. Appl. Phys. **46**, L559 (2007).
[22] J. Fünfschilling and M. Schadt, Jpn. J. Appl. Phys. **30**, 741 (1991).
[23] A. Jákli, S. Markscheffel, and A. Saupe, J. Appl. Phys. **79**, 1891 (1996).
[24] J. Prakash, A. Choudhary, S. Kaur, D. S. Mehta, and A. M. Biradar, Phys. Rev. E **78**, 021707 (2008).
[25] S. Kaur, A. K. Thakur, R. Chauhan, S. S. Bawa, and A. M. Biradar, J. Appl. Phys. **96**, 2547 (2004).
[26] A. K. Thakur, S. Kaur, S. S. Bawa, and A. M. Biradar, Appl. Opt. **43**, 5614 (2004).
[27] A. Mukherjee, M. Rahman, S. S. Bhattacharyya, B. K. Chaudhuri, and A. Yoshizawa, Chem. Phys. Lett. **443**, 71 (2007).
[28] G. Hegde, P. Xu, E. Pozhidaev, V. Chigrinov, and H. S. Kwok, Liq. Cryst. **35**, 1137 (2008).
[29] J. Fünfschilling and M. Schadt, J. Appl. Phys. **66**, 3877 (1989).
[30] A. Choudhary, A. Bawa, Rajesh, S. P. Singh, and A. M. Biradar, Phys. Rev. E **95**, 062702 (2017).
[31] L. K. Gangwar, A. Bawa, A. Choudhary, S. P. Singh, Rajesh, and A. M. Biradar, Phys. Rev. E **97**, 062707 (2018).
[32] A. Bawa, A. Choudhary, A. K. Thakur, S. Kumar, Rajesh, S. P. Singh, and A. M. Biradar, Appl. Phys. A **126**, 171 (2020).
[33] A. Bawa, L. K. Gangwar, A. Dhingra, A. Choudhary, S. P. Singh, W. Haase, and A. M. Biradar, Liq. Cryst. **46**, 166 (2019).
[34] W. Haase and S. Wróbel (eds.), *Relaxation Phenomena* (Springer, Berlin/Heidelberg, 2003).
[35] M. B. Pandey, R. Dhar, V. K. Agrawal, R. Dabrowski, and M. Tykarska, Liq. Cryst. **31**, 973 (2004).
[36] M. Gupta, R. Dhar, V. K. Agrawal, R. Dabrowski, and M. Tykarska, Phys. Rev. E **72**, 021703 (2005).
[37] A. Bawa, T. K. Lamba, A. Choudhary, G. Singh, Rajesh, S. P. Singh, and A. M. Biradar, J. Mol. Liq. **302**, 112332 (2020).
[38] H. Takezoe, K. Kondo, K. Miyasato, S. Abe, T. Tsuchiya, A. Fukuda, and E. Kuze, Ferroelectrics **58**, 55 (1984).

Correction: A second affiliation was added for the fifth and sixth authors. The order of the first and second affiliations have now been set right.